Research article

Mingyang Su, Xueyu Chen, Linwei Tang, Bo Yang, Haijian Zou, Junmin Liu, Ying Li*, Shuqing Chen and Dianyuan Fan

Black phosphorus (BP)–graphene guided-wave surface plasmon resonance (GWSPR) biosensor

https://doi.org/10.1515/nanoph-2020-0251
Received April 23, 2020; accepted July 23, 2020; published online August 21, 2020

Abstract: Due to lower out-of-plane electrical conductance, black phosphorus (BP) provides a suitable host material for improving the sensitivity of biosensors. However, BP oxidizes easily, which limits practical applications. In this article, we propose a sensitivity-enhanced guided-wave surface plasmon resonance (GWSPR) biosensor based on a BP–graphene hybrid structure. This BP–graphene hybrid structure exhibits strong anti-oxidation properties and exceptional biomolecule-trapping capability, which improve the stability and sensitivity of GWSPR biosensors, respectively. We show that the proposed GWSPR biosensor can distinguish refractive indices in the range of 1.33–1.78 RIU (RIU is the unit of RI), and the sensitivity reaches a maximum of 148.2°/RIU when the refractive index of sensing target is 1.33 RIU. The high sensitivity and broad detection range indicate that the proposed biosensor could significantly impact fields such as biological and chemical detection.

Keywords: biosensor; black phosphorus; graphene; hybrid structure; surface plasmon resonance.

***Corresponding author: Ying Li**, International Collaborative Laboratory of 2D Materials for Optoelectronics Science & Technology of Ministry of Education, Engineering Technology Research Center for 2D Material Information Function Devices and Systems of Guangdong Province, Institute of Microscale Optoelectronics, Shenzhen University, Shenzhen 518060, China, E-mail: queenly@szu.edu.cn. https://orcid.org/0000-0002-3950-1473
Mingyang Su, Xueyu Chen, Linwei Tang, Bo Yang, Haijian Zou, Shuqing Chen and Dianyuan Fan, International Collaborative Laboratory of 2D Materials for Optoelectronics Science & Technology of Ministry of Education, Engineering Technology Research Center for 2D Material Information Function Devices and Systems of Guangdong Province, Institute of Microscale Optoelectronics, Shenzhen University, Shenzhen 518060, China. https://orcid.org/0000-0002-2321-4760 (S. Chen)
Junmin Liu, College of New Materials and New Energies, Shenzhen Technology University, Shenzhen 507738, China

1 Introduction

Surface plasmons are localized waveguide modes that propagate metal surfaces and are produced by coupling electromagnetic waves with electrons [1]. Once the momentum between the incident photons and surface plasmons is matched by manipulating the incidence angle, surface plasmon resonance (SPR) appears, and the reflected light will significantly decay [1, 2]. Because the SPR effect is sensitive to the refractive index (RI) of the sensing target, the changes of RI will lead to a significant shift in the resonance angle, which enables an efficient way to distinguish RIs [3, 4]. Various biosensors that use the SPR effect have been widely applied in the fields of environmental monitoring [5, 6], medical diagnostics [7, 8], food safety [9, 10], and biochemistry [11, 12]. Among these biosensors, angle of incidence interrogation schemes are ubiquitous for detecting RIs but often suffer from low sensitivity [13–15]. To increase sensitivity, a silicon (Si) film can be coated on the metal surface to build guided-wave surface plasmon resonance (GWSPR) biosensors. Silicon is ideal because of its high RI and ease of deposition. Because the SPR effect is sensitive to analytes with high RI, the silicon film can interact with the sensing target to improve the effective RI of analytes [16]. To achieve high sensitivity, the coupling prism with low RI is required because the variation of resonance angle increases with the decrease of coupling prims' RI, which results in enhanced sensitivity. However, this coupling prism will reduce the detection range because of the increased resonance angle [15]. Hence, there appears to be a trade-off between sensitivity and detection range.

Apart from significantly altering the detection mechanism, optical materials with a high sensing capacity can be used to greatly enhance the sensitivity of GWSPR biosensors [17, 18]. Two-dimensional (2D) materials, such as graphene [19], transition metal dichalcogenides (TMDCs) [20], topological insulators [21], and black phosphorus (BP) [22], have been widely studied in biosensors for their high biocompatibility and biomolecule-trapping capability. Recently, graphene and TMDCs have been introduced to

SPR biosensors to improve sensitivity and more than twice the sensitivity was achieved [23, 24]. But the sensing performance is limited because these 2D materials have a large extinction coefficient, which could cause unwanted energy loss [24]. Compared with conventional 2D materials, BP has a relatively small extinction coefficient, which can be used to minimize loss. Additionally, they have a high molecular adsorption energy that makes it ideal for trapping biomolecules [25, 26]. And BP also has a more sensitive response to the target analytes, and the natural sensing capacity is about ~20 times than MoS_2 like 2D materials because of the high molar response factor [27]. These advantages suggest that BP is a suitable material for GWSPR biosensors. However, BP will oxidize in natural environments, which makes BP-based biosensors intrinsically instable [28].

BP–graphene hybrid structures have attracted significant attention because they retain BP's optoelectronic characteristics and address the oxidation problem. By coating graphene on the surface of BP, a bilayer structure with stable carbon-based atomic rings is formed. This structure separates the BP from air, which not only reduces the oxidation of BP but also maintains its sensitive response to target analytes [29–31]. Hence, we propose and investigate a BP–graphene hybrid structure GWSPR biosensor. It has an excellent detection capability for the medium with the RI ranges from 1.33 to 1.78 RIU (RIU is the unit of RI). By adjusting the number of BP layers and the thickness of Si films, the sensitivity reaches a maximum of 148.2°/RIU when the RI of the sensing target is 1.33 RIU. These results imply that this BP–graphene GWSPR biosensor breaks the long-standing trade-off between sensitivity and detection range, which may greatly enhance applications in biological sensing, medical detection, and biochemistry.

2 Structural design and theoretical analysis

Figure 1 shows the schematic of the GWSPR biosensor. As shown in Figure 1a, a chalcogenide (2S2G) glass is chosen as the coupling prism, an aluminum (Al) film (35 nm) is employed as the metal layer for exciting Surface Plasmon Polaritons (SPP), and a Si film (d_{Si} = 14 nm) is used as the substrate layer. Then, BP is coated on the surface of the Si film, and a graphene layer is covered on the BP layers as the molecular recognition element. The thickness of BP is $d_{BP} = L \times 0.53$ nm, where the thickness of monolayer BP is 0.53 nm, and L is the number of BP layers. The thickness of graphene is $d_G = S \times 0.34$ nm, where the thickness of monolayer graphene is 0.34 nm, and S is the number of graphene layers. Figure 1b describes the working schematic diagram. As shown in Figure 1b, the Transverse Magnetic (TM)-polarized light with the wavelength of λ = 633 nm is used as an exciting source because the SPR effect can just be excited by TM polarization [1–3], and the BP–graphene hybrid structure is used to enhance the sensitivity of the biosensor. Because of the carbon-based atomic rings, biomolecules will be adsorbed on the surface of BP–graphene hybrid structure [3], and the resonance angle of biosensor will change with sensing targets, which can be used to detect the RI shift.

The coupling prism is designed by 2S2G, which is an isotropic material, and its RI can be expressed as follows [32]:

$$n_{2S2G} = 2.24047 + \frac{2.693 \times 10^{-2}}{\lambda^2} + \frac{8.08 \times 10^{-3}}{\lambda^4} \quad (1)$$

where λ is the wavelength of incident light.

With the Drude–Lorentz model, the RI of the Al film can be expressed as follows [33]:

$$n_{Al} = 1 - \frac{\lambda\lambda_c^2}{\lambda_p^2(\lambda_c + i\lambda)} \quad (2)$$

where $\lambda_p = 1.0657 \times 10^{-7}$ m and $\lambda_c = 2.4511 \times 10^{-5}$ m, which are the plasma and collision wavelengths of Al, respectively.

The RI of graphene in the visible range is estimated to be $n_G = 3.0 + iC_1\lambda/3$, where $C_1 \approx 5.446$ μm^{-1}, and λ is the wavelength [34]. The few-layer BP can be approximately regarded as an isotropic material at the working wavelength of 633 nm where BP is polarization independent, and its RI is $n_{BP} = 3.5 + 0.01i$ [26, 35, 36].

Here, we use the transfer matrix method to simulate the optical field. All layers are perpendicularly stacked to the prism. Each layer is defined with the thickness d_k, dielectric constant ε_k, and refractive index n_k. The first tangential fields and the final boundary are set as $Z = Z_1 = 0$ and $Z = Z_{N-1}$, respectively. Their relationship can be given as follows [37]:

$$\begin{bmatrix} U_1 \\ V_1 \end{bmatrix} = M \begin{bmatrix} U_{N-1} \\ V_{N-1} \end{bmatrix} \quad (3)$$

where U_1 and V_1 are the tangential components of electric and magnetic fields at the boundary of first layer, respectively. U_N and V_N represent the Nth layer. M is the transfer matrix of the designed structure, which can be expressed as follows [37]:

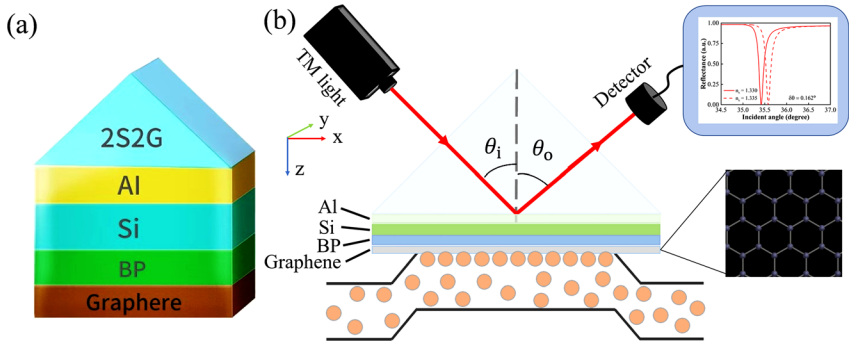

Figure 1: Scheme diagram of the guided-wave surface plasmon resonance (GWSPR) biosensor with a BP–graphene hybrid structure. (a) Structure and (b) work principle of the GWSPR biosensor. BP, black phosphorus.

$$M = \prod_{k=2}^{N-1} M_k = \begin{bmatrix} M_{11} & M_{12} \\ M_{21} & M_{22} \end{bmatrix} \tag{4}$$

$$M_k = \begin{bmatrix} \cos\beta_k & (-i\sin\beta_k)/q_k \\ -iq_k\sin\beta_k & \cos\beta_k \end{bmatrix} \tag{5}$$

where θ_{in} is the incident angle $q_k = (\varepsilon_k - n_k^2\sin^2\theta_{in})^{1/2}/\varepsilon_k$, and $\beta_k = 2\pi d_k/\lambda(\varepsilon_k - n_1^2\sin^2\theta_{in})^{1/2}$. Hence, the amplitude reflection coefficient can be inferred as follows [38]:

$$r_p = \frac{(M_{11} + M_{12}q_N)q_1 - (M_{21} + M_{22}q_N)}{(M_{11} + M_{12}q_N)q_1 + (M_{21} + M_{22}q_N)} \tag{6}$$

Finally, the reflectance (R) of the structure is given by the following equation:

$$R = |r_p|^2 \tag{7}$$

Because the resonance angle changes with the RI of sensing targets (n_s), the sensitivity of the GWSPR biosensor can be defined as $S = d\theta/dn_s$.

3 Results and analysis

3.1 Performance of the GWSPR biosensor

Sensitivity, detection range, and figure-of-merit (FOM) are the fundamental parameters to measure the performance of biosensors. Sensitivity is the responsivity of biosensors in sensing targets, detection range corresponds to the detected RI area of sensing targets, and FOM refers to the detection accuracy of SPR biosensors, which can be expressed as FOM = S/FWHM, where the FWHM is the full width at half maximum. High sensitivity and FOM are required to achieve the effective identification of sensing targets. Here, we will discuss the sensitivity, detection range, and FOM of the biosensor.

To evaluate the sensitivity performance, we compared three different structures: a SPR, a GWSPR, and the BP–graphene hybrid structure GWSPR biosensor. The reflectance of various structures as the function of incident angles is shown in Figure 2. Conventional SPR biosensors often have a typical structure of which the prism is covered by a single metal film, as shown in Figure 2a [32]. For comparison, an Al thin film is used as the metal film with a thickness of 35 nm, where the maximum reflectance with the corresponding resonance angle is obtained. Figure 2a shows the reflectance evolution as incident angles with n_s = 1.330 RIU and n_s = 1.335 RIU (the RI of sensing target), respectively. From the figure, the resonance angle changes ~0.162° when n_s varies from 1.330 to 1.335 RIU. Therefore, the sensitivity of SPR biosensors is estimated to be 32.4°/RIU. Also, we designed a GWSPR biosensor, and a sensitivity of 51.8°/RIU is obtained when a Si film with a thickness of 14 nm is coated on the Al film, indicating that the GWSPR structure can enhance the sensitivity of SPR biosensors, as shown in Figure 2b [24]. As presented in Figure 2c, when a BP monolayer is covered on the Si film, the resonance angles shift by 0.267°, and the sensitivity increases to 53.4°/RIU, which indicates that BP can increase the sensitivity of GWSPR biosensor. To reduce the oxidation of BP, graphene is coated on the surface of BP to form the BP–graphene hybrid structure. Graphene has excellent oxidizing resistance because of the strong in-plane sp^2 hybridization bonds in the honeycomb lattice [39]. Overcoming interface defects, graphene is easy to be combined with BP to form BP–graphene hybrid structures through the chemical bonding of phosphorus and carbon (P–C) [40]. This structure separates the BP from air, which not only reduces the oxidation of BP but also maintains its sensitive response to target analytes [29–31]. Figure 2d shows the reflectance curves with the numbers of BP and graphene layers are L = 1 and S = 1, and the sensitivity of 54.2°/RIU is obtained. The comparison of the resonance angle changes and sensitivities of above four biosensors are shown in Table 1. We found that the resonance angle shifts in the BP–graphene hybrid structure are larger than that in traditional SPR and GWSPR structures due to its

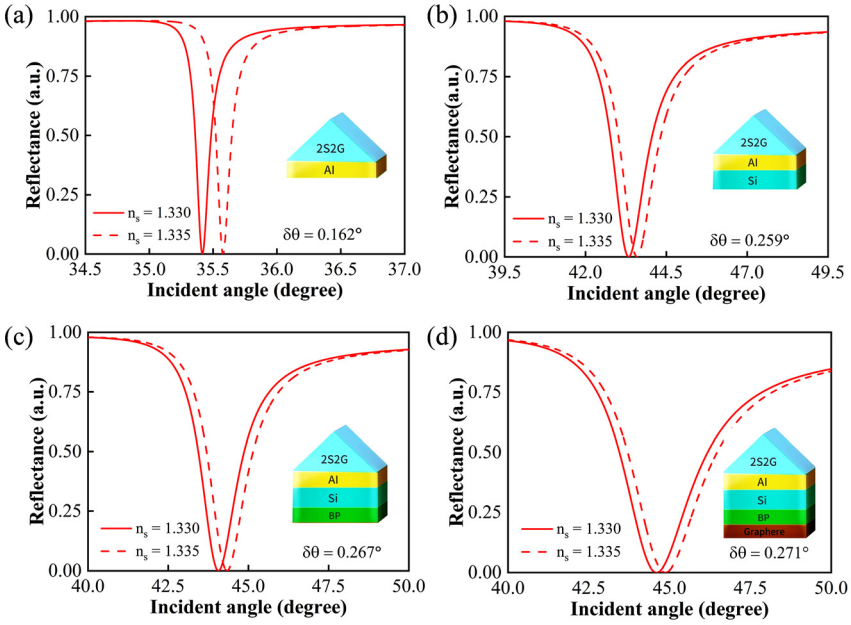

Figure 2: Reflectance of various structures as the function of incident angles. (a) Surface plasmon resonance (SPR) biosensor composed of chalcogenide (2S2G) coupling prism and aluminum (Al) film; (b) guided-wave surface plasmon resonance (GWSPR) biosensor composed of a silicon (Si) film with a thickness of 14 nm on the Al film; (c) black phosphorus (BP)–based GWSPR biosensor covering a BP monolayer on the surface of GWSPR biosensor; (d) proposed GWSPR biosensor coating a BP monolayer and a graphene monolayer on the surface of GWSPR biosensor.

Table 1: Resonance angle changes and sensitivities of four biosensors when the RI of sensing target is 1.33 RIU.

Biosensor structure	SPR	GWSPR	BP GWSPR	BP–graphene GWSPR
Resonance angle changes	0.162°	0.259°	0.267°	0.271°
Sensitivity	32.4°/RIU	51.8°/RIU	53.4°/RIU	54.2°/RIU

SPR, surface plasmon resonance; GWSPR, guided-wave surface plasmon resonance; BP GWSPR, black phosphorus guided-wave surface plasmon resonance.

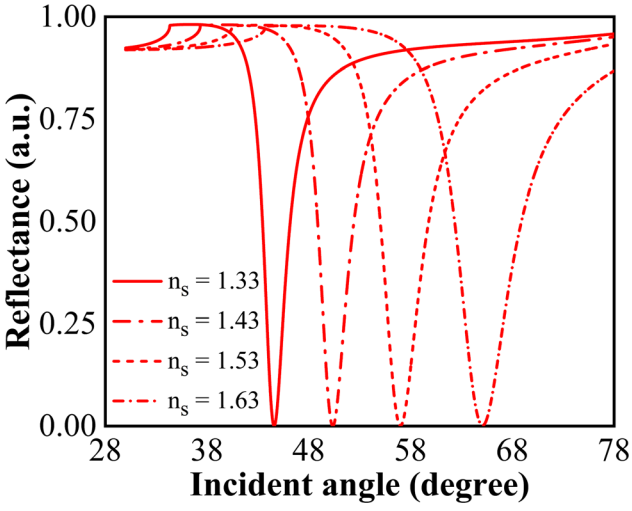

Figure 3: Reflectance curves change with incident angles for different sensing targets (different refractive indices [RIs]) where the thickness of silicon (Si) films is 14 nm, and the number of the black phosphorus (BP) and graphene layers is $L = 1$ and $S = 1$, respectively.

excellent sensitive response to target analytes. Hence, we conclude that the BP–graphene hybrid structure can enhance the sensitivity of GWSPR biosensors.

To evaluate the RI detection range, we investigated the reflectance curves under different sensing targets, as shown in Figure 3. The GWSPR biosensor can detect the RI of 1.33 RIU (RI of water is 1.33 RIU, which can be used to dissolve biomolecules) and be applied to identify other sensing targets. Generally, the resonance angles shift to larger angles as the RI increases. The resonance angles are 44.596°, 50.360°, 57.006°, and 65.074° for n_s = 1.33, 1.43, 1.53, and 1.63, respectively. Because only a small variation in the RI induces a large shift in the resonance angle, the biosensor can be used to detect a broad range of RIs.

The FOM is another critical parameter, which describes the resolution of biosensors. We plotted the evolution of sensitivity and FOM as the increase of RI, where the number of the BP and graphene layers is L = 1 and S = 1, respectively, and the results are presented in Figure 4a. As the RI increases from 1.33 to 1.78 RIU, the sensitivity will increase first and then decrease. The peak sensitivity of 189.6°/RIU appears at RI = 1.77 RIU. As shown in Figure 4a, the FOM decreases slowly first and then increases sharply. A minimum value of 14.68 appears when RI = 1.665. This phenomenon may be caused by the growth rate difference between the sensitivity and FWHM. The sensitivity enhancement is larger than the FWHM if the RI larger than

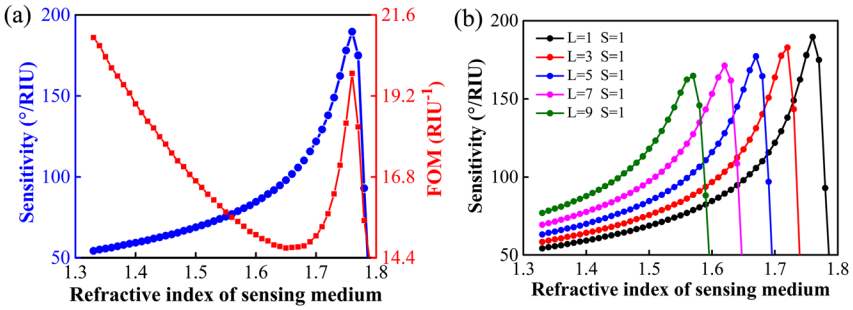

Figure 4: (a) Sensitivity and figure-of-merit (FOM) change with the refractive indices (RIs) of sensing targets where the thickness of silicon (Si) films is 14 nm, and the number of the black phosphorus (BP) and graphene layers is $L = 1$ and $S = 1$, respectively; (b) sensitivity changes with BP layers where the thickness of Si films is 14 nm, and the number of graphene layers is $S = 1$.

1.665 RIU, which leads to a rapid increase of the FOM. From Figure 4a, the biosensor can operate over a RI detection range of 1.33–1.78 with high sensitivity and FOM. Moreover, the sensitivity and detection range of the biosensor can be adjusted by changing the number of BP layers while keeping graphene unchanged, as shown in Figure 4b. The sensitivity enhances with the increase of BP layers while the RI detection range decreases, which means that the detection range of the proposed GWSPR biosensor can be controlled according to actual needs.

3.2 Geometry effect of the GWSPR biosensor

According to the discussion above, the number of BP layers has a positive effect on the performance of GWSPR biosensors. To obtain an optimum sensitivity, we further discuss the influence of BP/graphene layers and the thickness of Si film. Figure 5a shows the sensitivity versus the number of BP layers. The number of graphene layers is kept to $S = 1$, the thickness of Si film is 14 nm, and the RI of the sensing target is 1.33 RIU. As shown in Figure 5a, the sensitivity increases rapidly at first and then drops. When the number of BP layers is $L = 16$, an optimum sensitivity of 141.8°/RIU is obtained [32]. This can be explained as follows: as the continuous increase of BP layers, the resonance angle will move to 90°, but the detection angle cannot reach 90°. Thus, the sensitivity will drop. Figure 5b shows the sensitivity as the number of graphene layers increases, where the layer of BP is $L = 1$, and the thickness of Si film is 14 nm. Similar to the BP layers, an optimum sensitivity of 78.2°/RIU can also be obtained when the number of graphene layer is 22. However, the improvement of sensitivity is much smaller than that of increasing the BP layers. Through optimizing the number of BP layers and graphene layers, we obtain an optimum

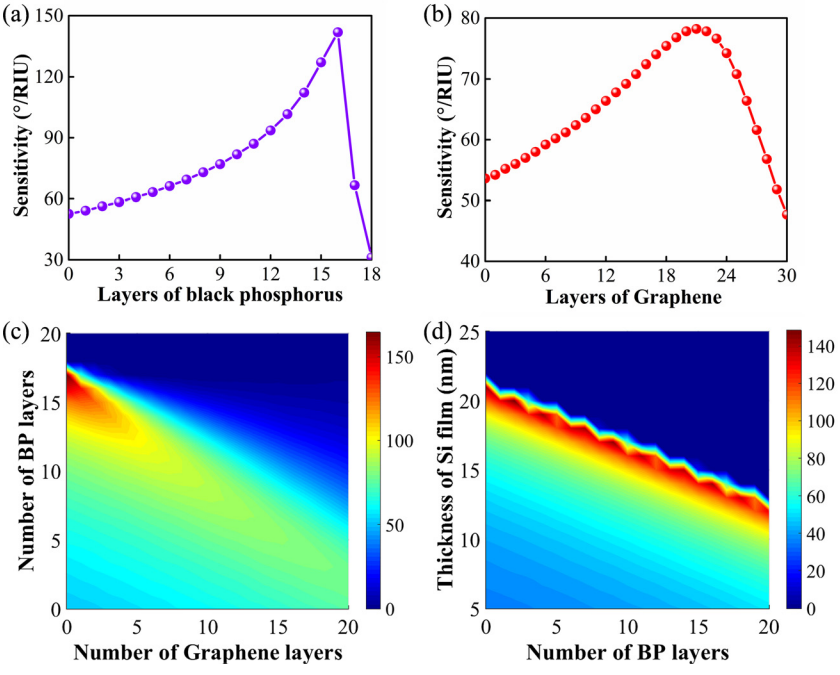

Figure 5: Sensitivity changes with various structure parameters when the refractive index (RI) of sensing target is 1.33 RIU, and the thickness of silicon (Si) film is 14 nm. (a) The number of the black phosphorus (BP) layers where the number of the graphene layers is $S = 1$; (b) number of the graphene layers where the number of the BP layers is $L = 1$; (c) number of the BP and graphene layers; (d) number of the BP layers and the thickness of Si film where the number of the graphene layers is $S = 1$.

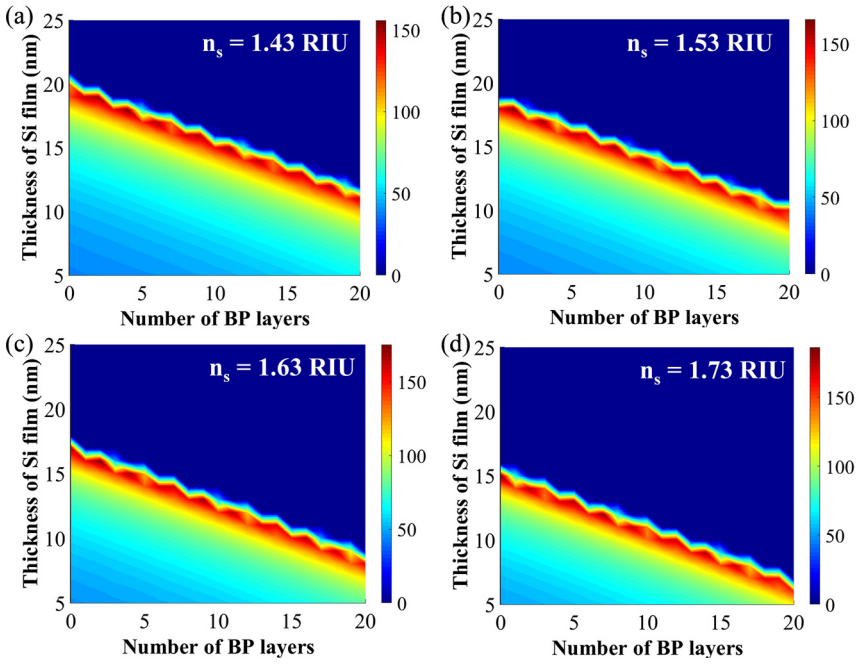

Figure 6: Sensitivity changes with the number of black phosphorus (BP) layers and the thickness of silicon (Si) film when the refractive index (RI) of sensing target is (a) 1.43 RIU, (b) 1.53 RIU, (c) 1.63 RIU, and (d) 1.73 RIU, where the number of the graphene layers is $S = 1$.

sensitivity of 141.8°/RIU at $L = 16$ and $S = 1$, as shown in Figure 5c. Evidently, the graphene does not significantly affect the sensitivity enhancement. The primary functions of the graphene are to defend BP from oxidation and to act as a macromolecular trapping mechanism. Through optimizing the number of BP layers and the thickness of Si film on sensitivity, we obtain an optimum sensitivity of 148.2°/RIU at $L = 2$ and $d_{Si} = 20$ nm, as shown in Figure 5d. Thus, to further enhance the sensitivity, the number of BP layers and the thickness of Si film must be simultaneously optimized. Furthermore, we discuss the combined effect of the number of BP layers and the thickness of Si films when the sensing targets have different RIs, as shown in Figure 6. The results show that the sensitivities with a specific RI can be optimized by adjusting the layer of BP and the thickness of Si film, and the optimum sensitivities are 155.2°/RIU, 166°/RIU, 175.2°/RIU, 186.2°/RIU with the RI of 1.43 RIU, 1.53 RIU, 1.63 RIU, 1.73 RIU, respectively, which are shown in Table 2.

Table 2: Sensitivities of the GWSPR biosensor with optimized BP layers and thickness of Si films for different sensing targets (different RIs).

RI	1.33	1.43	1.53	1.63	1.73
Number of BP layers	2	4	1	2	1
Thickness of Si film (nm)	20	18	18	16	14
Sensitivity (°/RIU)	148.2	155.2	166	175.2	186.2

RI, refractive index; BP, black phosphorus; GWSPR, guided-wave surface plasmon resonance.

3.3 Discussion

In this work, we propose a sensitivity-enhanced GWSPR biosensor based on the BP–graphene hybrid structure. The BP–graphene hybrid structure is coated on the surface of GWSPR biosensor to enhance the sensitivity because of the high antioxidant property and excellent sensitive response to target analytes. Different from other 2D material–based GWSPR biosensors, the sensitivity enhancement mainly attributes to the natural sensing properties of BP–graphene hybrid structure rather than the use of coupling prisms with low RI, making the GWSPR biosensor to have a broad detection range (RI ranges from 1.33 to 1.78). Because of the low out-of-plane electrical conductance, the maximum sensitivity of the proposed GWSPR biosensor is more than twice as the reported SPR biosensors that have broad detection ranges [33]. Moreover, the GWSPR biosensor can be designed with the actual need because the sensitivity and detection range can be controlled by increasing the BP layers.

The few-layer BP can be approximately regarded as an isotropic material at the working wavelength of 633 nm where BP is polarization independent. However, when the working wavelengths are in the 480 and 600 nm range, this biosensor is polarization dependent because of the anisotropy of few-layer BP caused by the RI difference in armchair (AC) and zigzag (ZZ) direction. To evaluate the anisotropy, we design the GWSPR biosensors with different working wavelengths and compare their reflectivity curves when the polarization of incident light is parallel to AC and

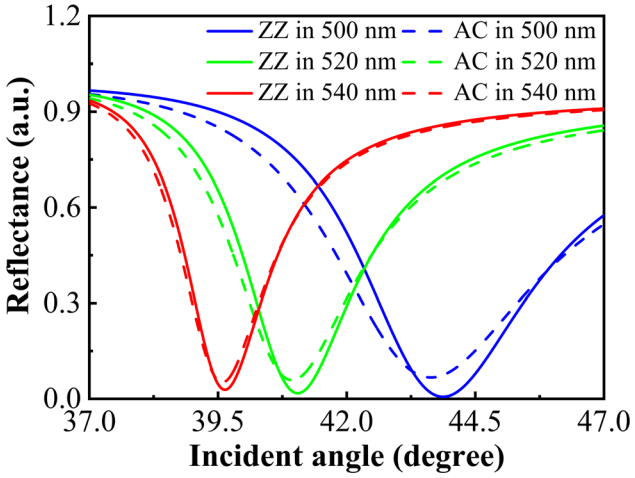

Figure 7: Shifts of the resonance angles when the polarization changes from zigzag (ZZ) to armchair (AC) directions.

ZZ direction. The results are shown in Figure 7. In the simulations, the number of graphene and BP layers is fixed as $S = 1$ and $L = 1$, while the thickness of Al and Si films is set as 35 and 7 nm, respectively. Figure 7 presents the reflectivity curves when the polarization of incident light is parallel to the AC and ZZ direction. As shown in Figure 7, the resonance angles shift from 43.76° to 43.63°, 41.05° to 40.94°, and 39.64° to 39.58° when the polarization changes from ZZ to AC direction with the wavelength of 500, 520, and 540 nm, respectively. It indicates the resonance angle relates to polarization, which may provide a possibility to detect sensing targets that has polarization-dependent RI.

4 Conclusion

In conclusion, we proposed a novel GWSPR biosensor with high sensitivity based on a BP–graphene hybrid structure. The number of BP layers and the thickness of Si films are used to adjust the sensitivity, while the graphene monolayer was applied as the macromolecular recognition element. The results show that the detection range of the proposed GWSPR biosensor ranges from 1.33 to 1.78, and the sensitivity improves with the increase of the RI of sensing mediums, which can be adjusted by increasing the BP layers if the RI detection range is satisfied. Besides, the optimum sensitivity of 148.2°/RIU is obtained, which is higher than that of the reported SPR biosensors that have broad detection ranges. It is indicated that the proposed biosensor has both the high sensitivity and broad detection range, which may have a potential perspective in optical sensing technology.

Acknowledgments: The National Natural Science Foundation of China (NSFC) (61805149 and 61805087); Guangdong Natural Science Foundation (2020A1515011392 and 2019A1515111153); Program of Fundamental Research of Shenzhen Science and Technology Plan (JCYJ20180507182035270); Science and Technology Planning Project of Guangdong Province (2016B050501005); Science and Technology Project of Shenzhen (ZDSYS201707271014468); and International Collaborative Laboratory of 2D Materials for Optoelectronics Science and Technology (2DMOST2018003) are acknowledged for their support by the authors.

Author contribution: All the authors have accepted responsibility for the entire content of this submitted manuscript and approved submission.

Research funding: National Natural Science Foundation of China (NSFC) (61805149 and 61805087); Guangdong Natural Science Foundation (2020A1515011392 and 2019A1515111153); Program of Fundamental Research of Shenzhen Science and Technology Plan (JCYJ20180507182035270); Science and Technology Planning Project of Guangdong Province (2016B050501005); Science and Technology Project of Shenzhen (ZDSYS201707271014468); and International Collaborative Laboratory of 2D Materials for Optoelectronics Science and Technology (2DMOST2018003) supported this work by providing research funding.

Conflict of interest statement: The authors declare no conflicts of interest regarding this article.

References

[1] L. M. Wu, J. Guo, H. L. Xu, X. Y. Dai, and Y. J. Xiang, "Ultrasensitive biosensors based on long-range surface plasmon polariton and dielectric waveguide modes," *Photon. Res.*, vol. 4, pp. 262–266, 2016.

[2] E. Kretschmann and H. Raether, "Notizen: radiative decay of nonradiative surface plasmons excited by light," *Z. Naturforsch. A.*, vol. 23, pp. 2135–2136, 1968.

[3] S. H. Choi, Y. L. Kim, and K. M. Byun, "Graphene-on-silver substrates for sensitive surface plasmon resonance imaging biosensors," *Opt. Express*, vol. 19, pp. 458–466, 2011.

[4] O. Salihoglu, S. Balci, and C. Kocabas, "Plasmon-polaritons on graphene-metal surface and their use in biosensors," *Appl. Phys. Lett.*, vol. 100, p. 213110, 2012.

[5] E. Mauriz, A. Calle, J. J. Manclús, A. Montoya, and L. M. Lechuga, "Multi-analyte SPR immunoassays for environmental biosensing of pesticides," *Anal. Bionanal. Chem.*, vol. 387, pp. 1449–1458, 2007.

[6] C. Hu, N. Gan, Y. Chen, L. Bi, X. Zhang, and L. Song, "Detection of microcystins in environmental samples using surface plasmon resonance biosensor," *Talanta*, vol. 80, pp. 407–410, 2009.

[7] J. W. Chung, S. D. Kim, R. Bernhardt, and J. C. Pyun, "Application of SPR biosensor for medical diagnostics of human hepatitis B virus (hHBV)," *Sens. Actuators B*, vol. 111, pp. 416–422, 2005.

[8] J. Ladd, A. D. Taylor, M. Piliarik, J. Homola, and S. Jiang, "Label-free detection of cancer biomarker candidates using surface plasmon resonance imaging," *Anal. Bioanal. Chem.*, vol. 393, pp. 1157–1163, 2009.
[9] J. Homola, J. Dostálek, S. Chen, A. Rasooly, S. Jiang, and S. S. Yee, "Spectral surface plasmon resonance biosensor for detection of staphylococcal enterotoxin B in milk," *Int. J. Food Microbiol.*, vol. 75, pp. 61–69, 2002.
[10] A. Rasooly, "Surface plasmon resonance analysis of staphylococcal enterotoxin B in food," *J. Food Protect.*, vol. 64, pp. 37–43, 2001.
[11] C. Ciminelli, C. M. Campanella, F. Dell'Olio, C. E. Campanella, and M. N. Armenise, "Label-free optical resonant sensors for biochemical applications," *Prog. Quantum Electron.*, vol. 37, pp. 51–107, 2013.
[12] D. Conteduca, F. Dell'Olio, F. Innone, C. Ciminelli, and M. N. Armenise, "Rigorous design of an ultra-high Q/V photonic/plasmonic cavity to be used in biosensing applications," *Opt. Laser Technol.*, vol. 77, pp. 151–161, 2016.
[13] A. Shalabney and I. Abdulhalim, "Sensitivity-enhancement methods for surface plasmon sensors," *Laser Photon. Rev*, vol. 5, pp. 571–606, 2011.
[14] L. Wang, Y. Sun, J. Wang, et al., "Sensitivity enhancement of SPR biosensor with silver mirror reaction on the Ag/Au film," *Talanta*, vol. 78, pp. 265–269, 2009.
[15] R. Tabassum and B. D. Gupta, "Performance analysis of bimetallic layer with zinc oxide for SPR-based fiber optic sensor," *J. Lightwave Technol.*, vol. 33, pp. 4565–4571, 2015.
[16] A. Lahav, M. Auslender, and I. Abdulhalim, "Sensitivity enhancement of guided-wave surface-plasmon resonance sensors," *Opt. Lett.*, vol. 33, pp. 2539–2541, 2008.
[17] L. Wu, H. S. Chu, W. S. Koh, and E. P. Li, "Highly sensitive graphene biosensors based on surface plasmon resonance," *Opt. Express*, vol. 18, pp. 14395–14400, 2010.
[18] K. V. Sreekanth, S. Zeng, K. T. Yong, and T. Yu, "Sensitivity enhanced biosensor using graphene-based one-dimensional photonic crystal," *Sens. Actuators B Chem.*, vol. 182, pp. 424–428, 2013.
[19] A. K. Geim and K. S. Novoselov, "The rise of graphene," *Nat. Mater.*, vol. 6, pp. 183–191, 2007.
[20] Q. H. Wang, K. Kalantar-Zadeh, A. Kis, J. N. Coleman, and M. S. Strano, "Electronics and optoelectronics of two-dimensional transition metal dichalcogenides," *Nat. Nanotechnol.*, vol. 7, pp. 699–712, 2012.
[21] H. Zhang, C. X. Liu, X. L. Qi, X. Dai, Z. Fang, and S. C. Zhang, "Topological insulators in Bi_2Se_3, Bi_2Te_3 and Sb_2Te_3 with a single Dirac cone on the surface," *Nat. Phys.*, vol. 5, pp. 438–442, 2009.
[22] S. Pal, A. Verma, S. Raikwar, Y. K. Prajapati, and J. P. Saini, "Detection of DNA hybridization using graphene-coated black phosphorus surface plasmon resonance sensor," *Appl. Phys. A*, vol. 124, p. 394, 2018.
[23] R. Verma, B. D. Gupta, and R. Jha, "Sensitivity enhancement of a surface plasmon resonance based biomolecules sensor using graphene and silicon layers," *Sens. Actuators B Chem.*, vol. 160, pp. 623–631, 2011.
[24] Q. L. Ouyang, S. W. Zeng, L. Jiang, et al., "Sensitivity enhancement of transition metal dichalcogenides/silicon nanostructure-based surface plasmon resonance biosensor," *Sci. Rep.*, vol. 6, p. 28190, 2016.
[25] L. Kou, T. Frauenheim, and C. Chen, "Phosphorene as a superior gas sensor: selective adsorption and distinct I–V response," *J. Phys. Chem. Lett.*, vol. 5, pp. 2675–2681, 2014.
[26] N. Mao, J. Tang, L. Xie, et al., "Optical anisotropy of black phosphorus in the visible regime," *J. Am. Chem. Soc.*, vol. 138, pp. 300–305, 2016.
[27] S. Y. Cho, Y. Lee, H. J. Koh, et al., "Superior chemical sensing performance of black phosphorus: comparison with MoS_2 and graphene," *Adv. Mater.*, vol. 28, pp. 7020–7028, 2016.
[28] J. D. Wood, S. A. Wells, D. Jariwala, et al., "Effective passivation of exfoliated black phosphorus transistors against ambient degradation," *Nano Lett.*, vol. 14, pp. 6964–6970, 2014.
[29] J. S. Bunch, S. S. Verbridge, J. S. Alden, et al., "Impermeable atomic membranes from graphene sheets," *Nano Lett.*, vol. 8, pp. 2458–2462, 2008.
[30] X. Sun, Z. H. Lu, T. Gupta, et al., "Comparative study on the antioxidation behaviors of polycrystalline multilayer and single-crystalline monolayer graphene," *2D Mater.*, vol. 6, p. 015020, 2019.
[31] L. M. Wu, J. Guo, Q. K. Wang, et al., "Sensitivity enhancement by using few-layer black phosphorus–graphene/TMDCs heterostructure in surface plasmon resonance biochemical sensor," *Sens. Actuators B Chem.*, vol. 249, pp. 542–548, 2017.
[32] P. K. Maharana and R. Jha, "Chalcogenide prism and graphene multilayer based surface plasmon resonance affinity biosensor for high performance," *Sens. Actuators B Chem.*, vol. 169, pp. 161–166, 2012.
[33] A. K. Sharma and B. D. Gupta, "On the performance of different bimetallic combinations in surface plasmon resonance based fiber optic sensors," *J. Appl. Phys.*, vol. 101, p. 093111, 2007.
[34] M. Bruna and S. Borini, "Optical constants of graphene layers in the visible range," *Appl. Phys. Lett.*, vol. 94, p. 031901-3, 2009.
[35] B. Meshginqalam and J. Barvestani, "Performance enhancement of SPR biosensor based on phosphorene and transition metal dichalcogenides for sensing DNA hybridization," *IEEE Sens. J.*, vol. 18, pp. 7537–7543, 2018.
[36] Y. T. Zhao, S. W. Gan, G. H. Zhang, and X. Y. Dai, "High sensitivity refractive index sensor based on surface plasmon resonance with topological insulator," *Results Phys.*, vol. 14, p. 102477, 2019.
[37] W. N. Hansen, "Electric fields produced by the propagation of plane coherent electromagnetic radiation in a stratified medium," *JOSA*, vol. 58, pp. 380–388, 1968.
[38] P. K. Maharana, R. Jha, and S. Palei, "Sensitivity enhancement by air mediated graphene multilayer based surface plasmon resonance biosensor for near infrared," *Sens. Actuators B Chem.*, vol. 190, pp. 494–501, 2014.
[39] J. R. Hahn, "Kinetic study of graphite oxidation along two lattice directions," *Carbon*, vol. 43, pp. 1506–1511, 2005.
[40] D. T. Phan, I. Park, A. R. Park, C. M. Park, and K. J. Jeon, "Black P/graphene hybrid: a fast response humidity sensor with good reversibility and stability," *Sci. Rep.*, vol. 7, p. 10561, 2017.